Photochemical Conversion of the O-intermediate to 9-*cis*-Retinal-Containing Products in Bacteriorhodopsin Films

Andreas Popp,* Markus Wolperdinger,* Norbert Hampp,* Christoph Bräuchle,* and Dieter Oesterhelt‡
*Institute for Physical Chemistry, LMU, Sophienstrasse 11, D-80333 Muenchen, Germany; ‡Max-Planck Institute for Biochemistry, Am Klopferspitz 18A, D-82152 Martinsried, Germany

ABSTRACT The photochemical activity of the O-state was investigated in bacteriorhodopsin (BR) films containing wildtype BR at pH 6.5 in the presence of glycerol. The formation of a photoproduct of O with an absorption maximum at 490 nm and 9-*cis*-retinal configuration was found. This 490-nm product was named P and shows a slow thermal reaction into a compound with a maximal absorption at 380 nm which was named Q and contains free 9-*cis*-retinal in the proteins binding site. The photoproducts of O, i.e., P and Q, are very similar, or even identical, to those previously observed in blue membranes. Common to the O-state and blue membrane forms of bacteriorhodopsin is a protonated aspartic acid 85, and we suggest that it is the reduced negative charge around the Schiff base which is responsible for the 9-*cis* photoisomerization. The release of a proton from aspartic acid 85 is linked to the conversion of the O-state back to the initial state of BR. Therefore the conditions of low proton mobility in BR films containing glycerol favor the accumulation of the O-state. For optical and holographic applications such BR films are very attractive. It is possible to create photoproducts with red light which are thermally stable at room temperature and that can be photochemically erased. Dependent on the light composition both properties can be realized in the same sample material. This feature may bridge the gap between information processing and short-term and long-term storage of information with BR.

INTRODUCTION

The photochromic retinal protein bacteriorhodopsin (BR) is found in the cell membrane of the archaeon *Halobacterium salinarium* (formerly *Halobacterium halobium*) (Oesterhelt and Stoeckenius, 1971) where it acts as a light-driven proton pump. BR is the key protein for photosynthetic growth of *H. salinarium* and, together with the closely related light-driven chloride pump halorhodopsin, it enables halobacteria to survive in salt lakes with an inhospitable natural environment, i.e., at high salt concentration and low oxygen tension. The biophysical and biochemical properties of BR have been studied intensively in recent years and a detailed knowledge of its structure and function has resulted (for reviews see, e.g., Kouyama et al. (1988) and Birge (1990)). In the halobacterial cell membrane BR occurs in the form of a two-dimensional hexagonal crystalline lattice of BR trimers. Due to their intense color these patches are called purple membranes (PM). In the PM-state BR shows an astonishing stability toward chemical, thermal, and photochemical degradation which is lost after solubilization of the membrane (Baribeau and Boucher, 1985). The photochemical properties of BR (Harbison et al., 1984; Varo et al., 1990; Varo and Lanyi, 1991) are summarized in Fig. 1.

The availability of BR variants with modified amino acid sequences (Dunn et al., 1987; Nassal et al., 1987; Soppa et al., 1989; Soppa and Oesterhelt, 1989; Ni et al., 1990) has improved the understanding of the proton transport mechanism in BR significantly. In addition, a new impulse for technical applications of BR was created, since engineering of BR and thereby the modification of its photophysical properties has become feasible. The photochromic properties of BR and its variants provide recording media for optical and holographic information processing with superior quality (Oesterhelt et al., 1991; Bräuchle et al., 1991; Gross et al., 1992; Haronian and Lewis, 1991; Werner et al., 1992; Vsevolodov et al., 1986). It has been found that BR films containing the BR variant BR_{D96N}, which differs from the wild type (BR_{WT}) by the exchange of aspartic acid 96 for asparagine, show an improved light sensitivity and a substantially higher holographic diffraction efficiency than BR_{WT} films (Hampp et al., 1992).

The difference in the light sensitivity is due to the longer lifetime of the M-intermediate of BR_{D96N} which in turn is related to the loss of its internal molecular proton donor group (Miller and Oesterhelt, 1990). However, the observed differences in the maximal diffraction efficiencies, in particular at the wavelength 633 nm, were initially not obvious. Recently it has been shown that the pH-dependent steady-state population of the O-state (Varo et al., 1990) which differs between BR_{WT} and BR_{D96N} is the reason for the higher diffraction efficiencies of the BR_{D96N} films (Hampp et al., 1992). A detailed analysis of the holographic diffraction pattern which is observed with BR_{WT} films led to the assumption that a photochemical conversion of the O-state and the formation of side products of the standard photocycle must occur in these films.

In this paper we report on this photochemical conversion of the O-state into a product with an absorption maximum at 490 nm and 9-*cis* retinal configuration which we name P-state. It should be mentioned that there is no relation to the P-state introduced by Drachev et al. (1986), which revealed to be identical to the N-intermediate. The P-product introduced here undergoes a slow thermal reaction to a further

Received for publication 3 March 1993 and in final form 24 June 1993.
Address reprint requests to Dr. Norbert Hampp.

0006-3495/93/10/1449/11 $2.00

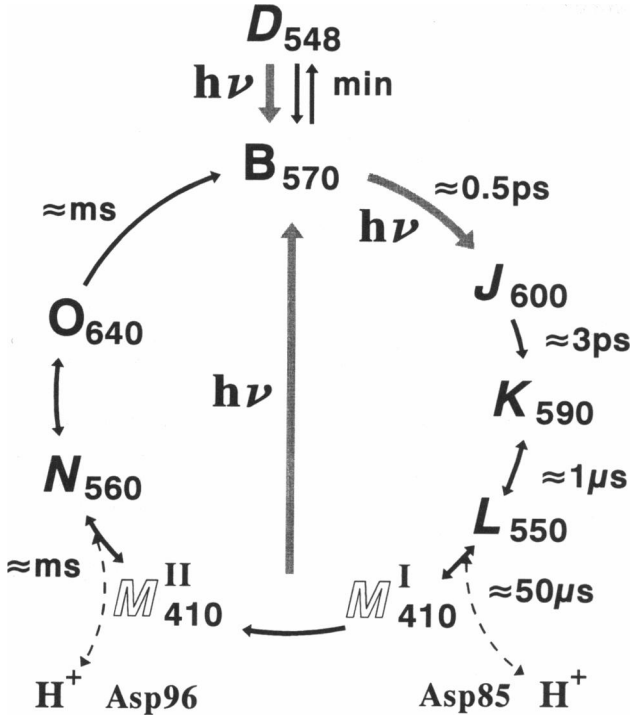

FIGURE 1 Simplified model of the photocycle of BR_{WT} in suspension. The BR-states are represented by single letters and their absorption maxima are given as indices. The states given in italics have a 13-*cis* configuration of the retinal, those in capital letters (*B* and *O*) contain all-*trans* retinal. Bold letters signify that the Schiff base is protonated, outlined letters (M^I and M^{II}) indicate a deprotonated form. The mixture of B (all-*trans*, 15-*anti*) and D (13-*cis*, 15-*syn*) which is obtained in the thermal equilibrium in the dark is called dark-adapted BR. Thermal steps are represented by black arrows, photochemical conversions by thick grey arrows.

blue-shifted product named Q with an absorption maximum at 380 nm which may be free 9-*cis*-retinal in the binding site. P and Q are similar or even identical to photoproducts formed from acidified purple membrane in glycerol (Maeda and Yoshizawa, 1980) and from the blue membrane (Fischer et al., 1981). Both O-photoproducts P and Q can be photochemically reconverted into the BR initial state and therefore provide a first example of a photostable, photoerasable BR-state at neutral pH.

EXPERIMENTAL PROCEDURES AND RESULTS

Preparation of BR films

BR_{WT} in the form of purple membranes was isolated from halobacterial strain S9 by the procedure described in (Oesterhelt and Stoeckenius, 1974). Glass plates with a thickness of 1 mm were used as substrates for the preparation of BR films. They were cleaned with acetone and siliconized twice with a solution of 3% dimethyldichlorosilane (DDS) in tetrachloromethane prior to use. Unbound DDS was removed by extensive washing with ethanol. A buffer stock solution (100 mM) was prepared from potassium phosphate (pH 6.5) in doubly distilled water. BR films with a thickness of approximately 25 μm were formed between two glass plates as described in (Hampp et al., 1992).

Retinal extraction and analysis of the isomer composition

Analysis of the isomer composition in BR films was done by retinal extraction in the dark and high-performance liquid chromatographic (HPLC) analysis (Steinberg et al., 1991; Scherrer et al., 1989). BR material was extracted twice with a cold mixture of isopropanol/*n*-hexane at pH 7.0 and analyzed on a Si60 column at a detection wavelength of 360 nm.

Steady-state absorbance changes in BR films: continuous wave excitation by two actinic wavelengths

The setup shown in Fig. 2 was used for the absorption measurements under continuous wave (cw) excitation. From the krypton 1 laser a pump beam is emitted and varied in its intensity by means of an acousto-optic modulator (AOM). The AOM has a contrast ratio of approximately 1000. A beam expander (BE) was used to enlarge the beam diameter and by use of an aperture (A) the inner part of the Gaussian beam profile was selected. Alternative to excitation by the krypton 1 laser the collimated beam (COL) from an arc lamp was band pass filtered (BF, 560 ± 30 nm) and was used for excitation of the BR film at a fixed intensity. This setup was chosen since the intensity of the probing beams can be kept very low.

The light-induced absorption changes were detected simultaneously by four monochromatic probe beams at selected wavelengths. The first was obtained by decoupling a

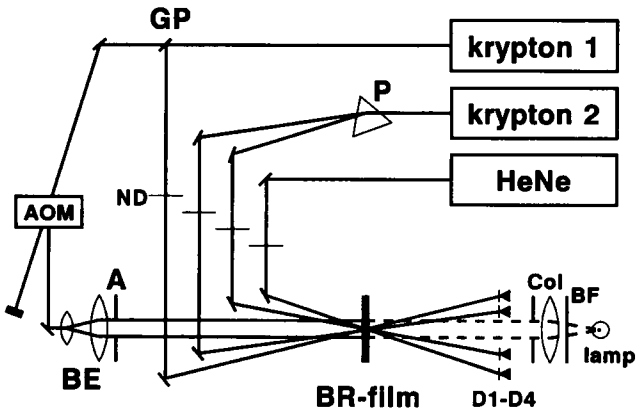

FIGURE 2 Experimental setup for the intensity-dependent absorption measurements. The acusto-optic modulator (AOM) is used to vary the intensity of the (actinic) pump beam emitted by krypton laser 1. The modulated beam is expanded (BE), the inner part of the Gaussian intensity profile is cut out by an apperture (*A*) and incidents to the BR film. A prism (*P*) is installed to separate the wavelengths emitted by krypton laser 2 which runs in multi-line mode. Two further test wavelengths are obtained from a HeNe Laser and by decoupling of a small fraction of the beam intensity of laser 1 by a glass plate (*GP*). An additional band pass filtered (*BF*) and collimated (*Col*) arc lamp (560 ± 30 nm) can be used to obtain an initial steady-state population of photocycle intermediates in the BR film prior to the intensity scan of the beam from laser 1. The intensities of the four test beams are adjusted by neutral density filters (*ND*). A set of four photodiodes (D1–D4) is used for the detection of the transmitted beams.

small fraction of the variable actinic (pump) beam out of the light path by means of a 10-mm-thick glass plate (GP). The other three beams were supplied by a second krypton laser (krypton 2) running in multi-line mode and a HeNe laser. All probe beams were incident to the BR film at an angle of ±8° relative to the (actinic) pump beam. Their intensities were adjusted by neutral density filters (ND) and were approximately 50 μW/beam. As wavelengths all available emission lines of the krypton lasers were used. The induced transmittance changes were monitored by a set of photodiodes (D1–D4) and recorded on a digital storage oscilloscope.

The absorbance changes of a BR_{WT} film of pH = 6.5 which had an initial optical density at 570 nm of iOD_{570} = 3.3 were analyzed at the wavelengths 413, 482, 568, and 633 nm and are plotted in Fig. 3. The absorption changes are given as percent of the initial absorption at the respective wavelengths and as a function of the intensity in the beam of the krypton 1 laser (see Fig. 2). The time for an intensity sweep between minimum and maximum was 80 s.

First beam 1 at 568 nm was raised from 0.5 to 300 mW/cm^2 (Fig. 3, left column) and an intensity-dependent decrease of the absorption at 568 and 482 nm and an increase at 633 and 413 nm was observed. This is related to the photochemical depopulation of the B-state and the appearance of intensity-dependent, steady-state populations of the M-, N-, and O-states. Second (Fig. 3, middle column), the BR film was continuously illuminated by the arc lamp (560 ± 30 nm) at an intensity of 87 mW/cm^2 and initially a population distribution of the B-, M-, N-, and O-states was produced. Then a second continuous beam at 413 nm was varied in its intensity from 2 to 500 mW/cm^2 (Fig. 2, krypton 1). With an increasing intensity of this blue beam the M-state became depopulated due to the photochemical conversion M → B (see Fig. 1). As expected the absorption in the blue region of the visible spectrum decreased and the B-dominated absorbance (568 and 482 nm) increased. Only very small changes of the absorption are observed in the red at 633 nm. In a third experiment (Fig. 3, right column) the kryp-

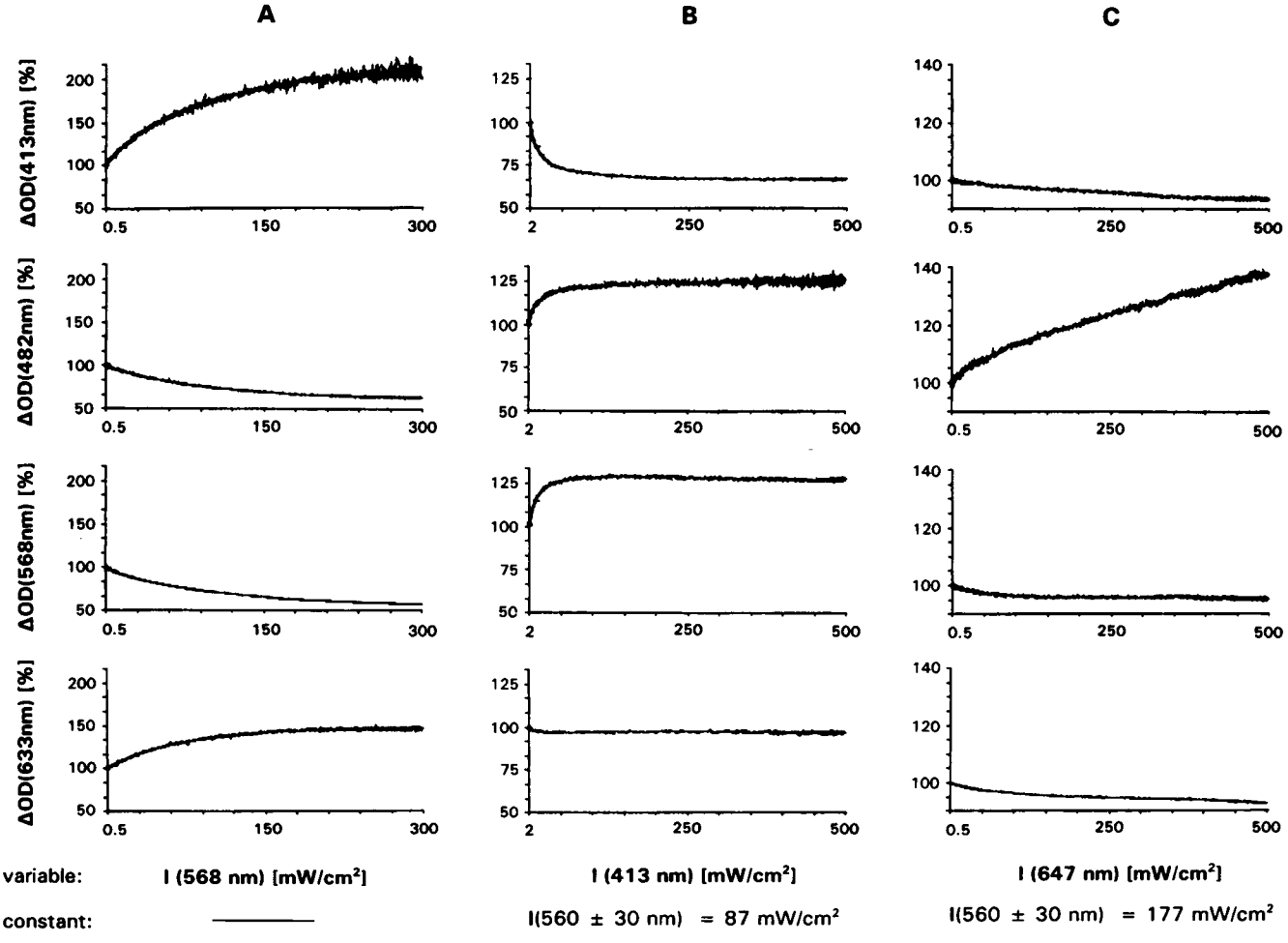

FIGURE 3 Intensity dependence of the steady-state absorption changes of a BR_{WT}-film with an initial optical density of iOD_{570} = 3.3 at pH 6.5 upon excitation with one or two wavelengths. On the *x*-axis the intensity of the variable pump beam is shown in bold letters. The intensity of the (optional) additional constant broad band excitation is indicated at the bottom. On the *y*-axis the induced changes of the optical density ΔOD normalized to the initial value at the indicated wavelengths are given in percent. The time for the intensity sweep was 80 s. Left column (*A*): intensity sweep from 0.5 to 300 mW/cm^2 with 568 nm. Middle column (*B*): constant broad band excitation (560 ± 30 nm) with 87 mW/cm^2 and sweep of the 413-nm intensity from 2 to 500 mW/cm^2. Right column (*C*): constant broad band excitation (560 ± 30 nm) with 177 mW/cm^2 and sweep of the 647 nm intensity from 0.5 to 500 mW/cm^2.

ton 1 beam had a wavelength of 647 nm and was varied from 0.5 to 500 mW/cm^2. At 413, 568, and 633 nm a slight decrease occurred but at 482 nm a significant increase of the absorption was observed. This indicates that a state which absorbs in the red can be photochemically converted into a product(s) which absorbs in the blue-green region. Note that the absorption changes are given as percent of the initial optical density iOD at the indicated wavelengths, emphasizing the rise of the new photoproduct shown in the right column of Fig. 3.

The spectral properties of this product were recorded by difference spectroscopy in the following way. Light-induced absorption changes were determined for all krypton emission wavelengths (Fig. 2, krypton 2) at a constant excitation with the arc lamp and switching the 647-nm excitation (Fig. 2, krypton 1) from 0.5 to 500 mW/cm^2. The absorption differences obtained are plotted in Fig. 4. In this difference spectrum the appearance of an absorption at 490 nm is observed. The negative features of the difference spectrum indicate the disappearance of M-state (ΔOD ~ 400 nm) and point out also the net loss of material absorbing around 600 nm under the photostationary conditions.

These experiments confirm that under illumination with 647 nm a photoproduct of BR is formed which absorbs in the blue-green region that will be called P. The educt BR-state from which the P-state is formed is not obvious from these measurements because the applied conditions produce a complex photochemical reaction pattern. However, from the absorption properties of the photocycle intermediates the red-shifted K- and O-state must be considered as possible educt BR-states. Since the steady-state concentration of the K-state is very low at room temperature the O-state seems to be the most likely candidate for the observed product. A stringent proof that the educt is not the B-state itself but one of the red absorbing photointermediates, i.e., the O-state, can be obtained by holographic techniques and is described in the following.

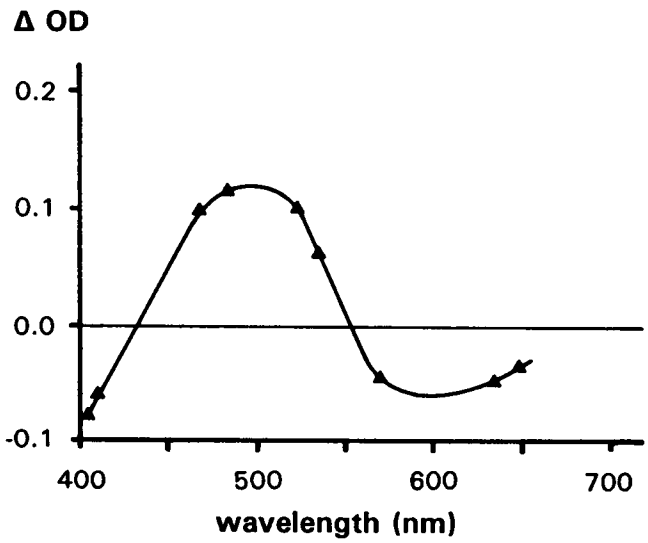

FIGURE 4 Difference spectrum obtained from a BR_{WT}-film of iOD_{570} = 3.3 and pH = 6.5, which is constantly illuminated with 177 mW/cm^2 of light of 560 ± 30 nm, which was induced by an 100-fold increase from 0.5 to 500 mW/cm^2 of simultaneous irradiation with 647 nm. Absorption changes were monitored at various wavelengths of the krypton 2 laser in Fig. 2. The high red light-intensity causes the formation of a product with an absorption maximum at about 490 nm.

Analysis of the phase and amplitude distribution of the diffracted wave from holographic gratings in BR films: O-type holograms

A more sensitive tool than the steady-state absorption measurements is the analysis of the amplitude and phase distribution of the holographic diffraction pattern. In particular it allows the distinction between a photoreaction starting from the B-state and photoreactions of intermediates of the photocycle as will be demonstrated by the results described below.

For analytical investigations it is reasonable to use the simplest hologram, i.e., a plane wave hologram. Due to the Gaussian intensity distribution of the recording beams the photochemistry occurring at different light intensities can be investigated in parallel when the spatial distribution of the phase and amplitude of the diffracted beam is analyzed.

For this purpose (see Fig. 5) a laser beam of variable wavelength from 468 to 647 nm (laser 1, krypton lines) with a Gaussian intensity distribution (TEM_{00}) is divided by a beamsplitter (BS) into two coherent beams of equal intensity. The intensity distribution $I(x, y)$ along the x and y axes of the interference pattern in the plane of the BR film is given by

$$I_w(x,y) = 2 \cdot I_{0w} \cdot \exp\left(-2\frac{x^2\cos^2\theta_w + y^2}{w_w^2}\right) \cdot [1 + \cos(2\pi x/G)] \quad \text{with} \quad G = \lambda_w/(2\sin\theta_w), \quad (1)$$

where I_{0w} is the maximal intensity of each of the writing beams (wavelength λ_w), G is the grating period, w_w their beam radii and $2 \cdot \theta_w$ the angle between them. From laser 2 a read/pump beam of wavelength λ_R = 521 nm which can be varied in its intensity by a variable neutral density filter (ND_{var}) incidents to the holographic grating at the Bragg angle $\theta_R = \arcsin(\lambda_R/2 \cdot G)$. This beam is diffracted at the grating formed in the BR film by the writing beams. A CCD-detector array connected to a monitor is placed in the path of the diffracted wave.

From the read/pump beam (521 nm) a fraction is decoupled by a semitransparent mirror (SM), adjusted in its intensity by neutral density filters (ND) to approximately the same intensity as the diffracted beam. It is superimposed with the diffracted beam on the CCD-detector array at a small angle, e.g., θ_D = 0.03°. The diffracted beam and this reference beam, which can be turned on and off by a shutter (SH), interfere because they are coherent and hence the phase distribution of the diffracted wave becomes visible.

In the bright parts of the intensity pattern resulting from the interference of the writing beams (see Eq. 1) the photochemical conversion of the B-state is initiated and concomitantly a population of the intermediate states appears. A

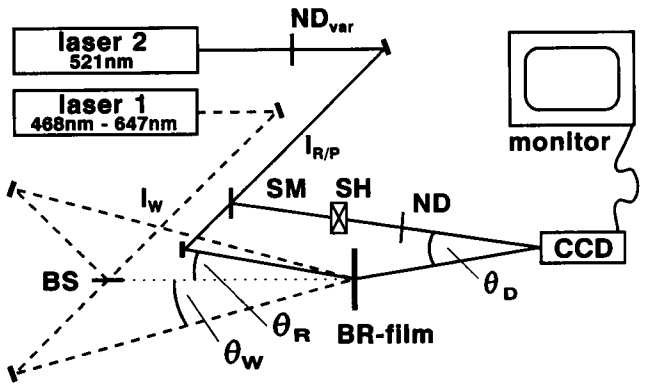

FIGURE 5 Holographic setup for the analysis of the phase distribution in the diffracted wave. Recording beams: λ_w = 647 nm, θ_w = 7.6°, I_{0w} = 358 mW/cm², w_w = 4 mm. Read/pump beam: λ_R = 521 nm, w_R = 4 mm. I_{0R} = 4–254 mW/cm². For definitions for w_R, w_w, I_{0w}, and I_{0R} see text. SM, semitransparent mirror; BS, beam splitter; ND_{var}, variable neutral density filter; ND, neutral density filter; SH, shutter.

description of the resulting modulation of the absorption coefficient and the refractive index and their contribution to the diffraction efficiency can be found, e.g., in Hampp et al. (1992), Bräuchle and Burland (1983), and Kogelnik (1969).

At low intensities of the read/pump beam (I_R) the fringe contrast of the holographic grating in the BR film is almost unaffected, therefore it can be considered as being non-actinic. At higher intensities the steady-state population of the different intermediates in the BR film are determined additionally by the intensity of the read/pump beam. Therefore, photochemical conversions of intermediates must be taken into account. This principle was first applied in so-called M-type holograms (Hampp et al., 1990).

In Fig. 6 the intensity-dependent transition of the Gaussian to a donut-shaped diffraction pattern with increasing intensities of the read/pump beam is shown. At a low intensity of the read/pump beam of I_R = 4 mW/cm² (Fig. 6 *A*) a Gaussian diffraction pattern is observed. A continuous transition to the donut-shape is found in parallel to the increase of the read/pump intensity (I_R = 50 mW/cm² in Fig. 6 *B*). The high intensity in the center of the read/pump beam leads to an erasure of the grating induced by the 647-nm writing beams due to saturation effects. Therefore, a weaker intensity is diffracted by this part of the sample causing the black spot in the center of the diffracted beam pattern (Fig. 6 *B*). Further increase in intensity of the read/pump beam causes another diffraction pattern specifically for the red part of the writing beams, e.g., 633, 647, and 676 nm. When the intensity of the read/pump beam (521 nm) is raised a steady increase of the diffracted intensity in the middle of the donut is observed (I_R = 254 mW/cm² in Fig. 6 *C*).

The characteristic transition from the gaussian to the donut-shape of the spatial intensity distribution of the diffracted wave (Fig. 6, *A* and *B*) is also found for writing wavelengths in the blue to yellow range, i.e., 468, 482, 531, and 568 nm. However the "filled donut" (Fig. 6 *C*) does not appear even at high read/pump intensities.

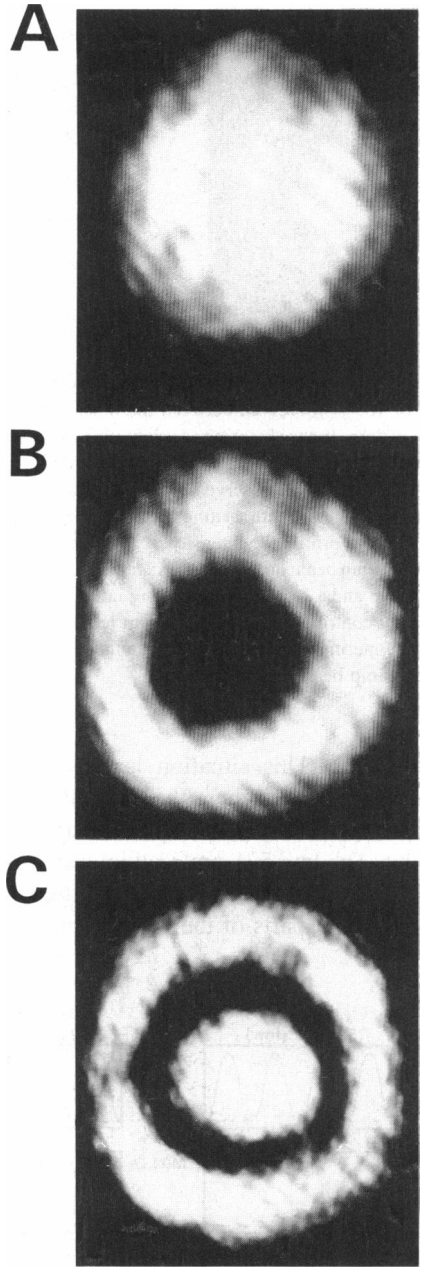

FIGURE 6 Spatial intensity distribution in the diffracted wave at different read/pump but constant writing intensities. Writing: λ_w = 647 nm, I_w = 328 mW/cm²; read/pump: λ_R = 521 nm, I_R: 4 mW/cm² (*A*), 50 mW/cm² (*B*), 254 mW/cm² (*C*).

In a next experiment the shutter (see Fig. 5) was opened and the phase distribution of the diffraction pattern was analyzed (Fig. 7). A comparison with Fig. 6 *C* shows that there is a phase shift between the outer ring and the center of the diffracted wave.

The wavelength dependence for the "filled donut" diffraction is the same as found in the absorbance measurements for the photochemical formation of P (Figs. 3 and 4). The intensity-dependent shift in the phase distribution indicates, that the hologram formation in the center is related to a photochemical conversion of an intermediate state in the

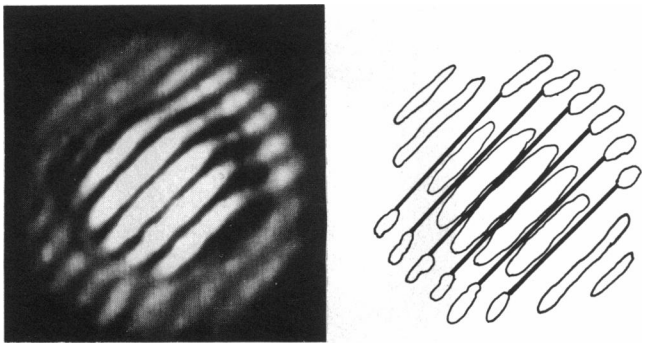

FIGURE 7 Phase distribution in the diffraction pattern shown in Fig. 6 *C*. A phase shift of 180° is observed between the inner and the outer part of the diffraction pattern. In the sketch on the right the bright parts of the outer ring are connected by thick lines. Since these lie in the dark parts of the inner grating a phase shift of 180° is observed. The outer ring relates to the B-type hologram formed by the 647-nm writing beams in the BR film where, due to the Gaussian beam profile the intensity of both the 647-nm writing and the 521-nm read/pump beam are low. In the central part where as well a high 521-nm read/pump and a high 647-nm writing intensity illuminate the BR film the dominant contribution to the hologram relates to a photochemical conversion of an intermediate which absorbs in the red and is populated by the continuous pump beam, i.e., the O-state.

photocycle of BR. This situation is explained schematically in Fig. 8. The case where the read intensity (521 nm) is low compared to the 647-nm write intensity (Fig. 8, *A1*) is treated first. The low 521-nm read intensity only induces a small population distribution change in the BR film (Fig. 8, *A2*). In the bright parts of the 647 nm intensity distribution a related photoconversion of the B-state occurs and the photointermediates M, N, and O are populated (*A3*). Since the read beam is almost nonactive this pattern is not altered when both the 521- and 647-nm intensities illuminate the film (*A4*). Even if a secondary photochemistry of the O-state occurs (products of O) no phase shift inside the grating results. In the second case the 521-nm intensity is high and therefore considered as actinic light (Fig. 8, *B1*). The 521-nm read/pump beam induces a corresponding and substantial population of the M-, N-, and O-states in the BR film (*B2*). The 647-nm intensity grating (*B3*) would be identical to that in (*A3*). The combined irradiance of the BR film with the 521 nm and the 647 nm intensities leads to a complex population distribution (*B4*). In the outer part of the irradiated area the B-type hologram is formed. In the middle the secondary photoreaction, i.e., the conversion of O to P now becomes dominant which results in the formation of an inversed grating. At the boundary a phase shift appears (*B4*).

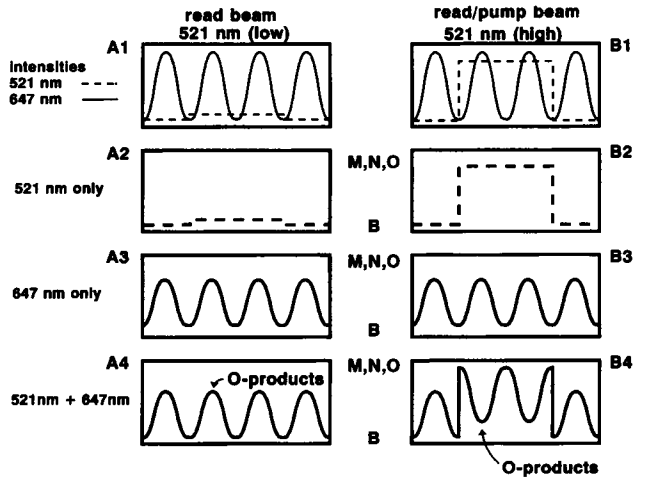

FIGURE 8 Scheme for the explanation of the phase-shift appearing in a holographic diffraction pattern where B-type and O-type holograms exist in parallel. (*left column*) A 647-nm intensity grating leads to a related B-type hologram without phase shift in the grating. (*right column*) Simultaneous illumination of a BR film with, e.g., 521 nm and 647 nm results in the outer part, where no 521 nm appears, in the formation of a B-type hologram. In the inner part, where initially a high steady-state population of intermediates is induced by the 521-nm read/pump beam, the conversion of photointermediates, in particular the O-state, dominates. This leads to an inversed hologram. At the boundary between the inner and outer part a phase shift of 180° appears.

From these experimental results the educt of the photochemical formation of P which absorbs at about 490 nm must be assigned to a photointermediate of the BR-photocycle. The only one which fulfills the spectroscopic characteristics and also reaches the required steady-state population is the O-state. Therefore we call these holograms O-type holograms in analogy to the M-type holograms reported earlier (Hampp et al., 1990).

Both have in common that the photochemical conversion of an intermediate of the BR-photocycle is used for recording which by definition is first populated by optical pumping of the BR film. M- and O-type holograms differ in the type of the photoproduct and in their holographic properties. In M-type recording the B-state is repopulated after photochemical excitation of the M-state with blue light. All the BR material is cycled within the first half of the photocycle, i.e., B $\rightleftarrows$ M. In the O-type holograms the photoreaction from O leads to a side product of the photocycle, i.e., P. Several questions arise: I) is P the only photoproduct? II) can P be reversibly converted to the initial B-state? III) does the back reaction take a thermal and/or a photochemical path? IV) is this reconversion via O?

A first observation clearly demonstrates the photochemical reversibility of the P formation. O-type holograms decay on a time scale of several tens of milliseconds when the writing beam (e.g., 647 nm) is turned off but the read/pump beam still irradiates the BR film. In the holographic experiments described so far a read/pump beam with a wavelength on the blue side of the B-state absorption was always used, e.g., 521 nm. This is within the absorption of P, or more precisely within the positive absorption change region of the difference spectrum in Fig. 4. From this we conclude that O-type holograms are erased photochemically. Therefore the chemical nature of the photoproduct(s) of O and their reconversion were investigated spectroscopically and their retinal configuration was analyzed.

Retinal configuration in the P and Q states and their photochemical conversion to the B state

In Fig. 9 the absorption changes accompanying the light-induced formation, the thermal conversion and light-stimulated reconversion of the photoproducts of O are shown. In the right row the related difference spectra are given. In parallel an analysis of the isomer composition was done by HPLC and the results are listed in Table 1.

First the photochemical formation of photoproducts of O with red light was analyzed. In Fig. 9 *A* the absorption spectrum of a BR_{WT}-film at pH 6.5 is shown before (I) and after 1, 2, and 3 min (II–IV) of illumination with 676 nm at an intensity of 830 mW/cm^2. The absorption in the maximum at 560 nm decreases and shifts slightly to 556 nm. This change is accompanied by an absorption increase around 450 nm, and a quasi-isosbestic point at 483 nm is observed. Retinal extraction and isomer composition analysis show that during this step 9-*cis*-retinal is formed (see Table 1, AI and AIV). The observed changes in the absorption spectra can be numerically simulated under the assumption that material absorbing at 560 nm is converted into two species which appear in a constant ratio of 30:70, one absorbing at 490 nm and the other absorbing at 560 nm. Since the 490-nm product found in the previous experiments alone cannot explain the observed quasi-isosbestic point at 483 nm, a third compound must be involved which is inactive with respect to the 560 → 490 nm transition but has its absorption maximum close to 560 nm. Since 11-*cis*-retinal was not found in the samples (Maeda and Yoshizawa, 1980) this compound contains presumably 13-*cis*-retinal which may be assigned either to the N-state or D-state (Kouyama et al., 1985).

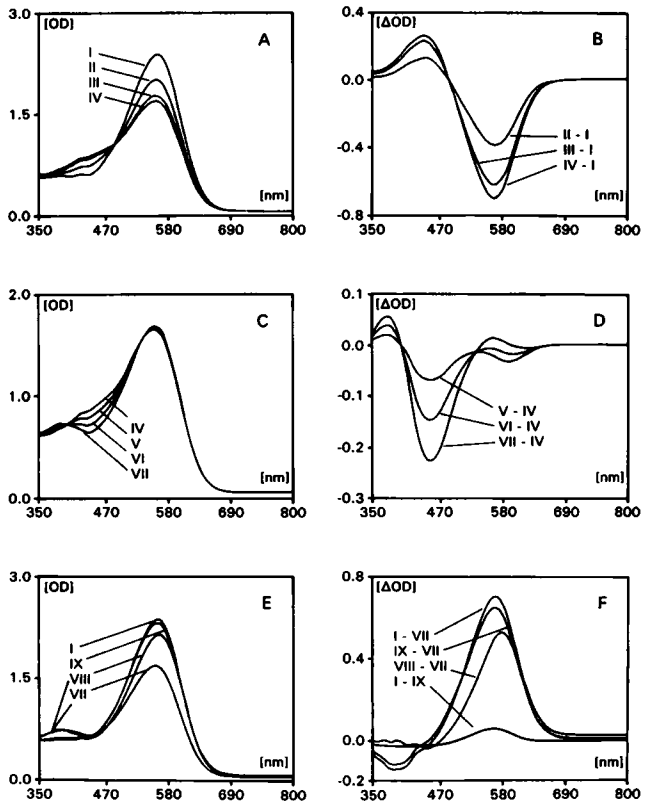

FIGURE 9 Photochemical conversion of the O-state and thermal and photochemical reactions of the products of O. In the left column the absorption spectra are shown for the formation and reconversion of the photoproduct(s) of O. In the right column the corresponding difference spectra are shown. (*A* and *B*) Photochemical formation: Spectra of a BR_{WT}-film (I) before and (II) after 1 min, (III) 2 min, and (IV) 3 min of illumination with 676 nm at an intensity of 830 mW/cm^2. (*C* and *D*) Thermal stability: Spectra of the BR film (IV) immediately after illumination and after (V) 1 h, (VI) 3 h, and (VII) 12 and 19 h in the dark. (*E* and *F*) Photochemical reconversion: Spectra of the BR film in state (VIII) after monochromatic illumination with 532 nm at 88 mW/cm^2 for 22 min (VIII) and (IX) after additional broad band excitation with an halogene lamp for 2 min at 400 mW/cm^2. The initial absorption spectrum (I) is given for comparison.

In the next step of the experiment the development of the system in the dark at room temperature was measured. The irradiated sample was kept in the dark and the absorption spectrum recorded over a period of 19 h. In Fig. 9 *C* the spectra after 0 (IV), 1 (V), 3 (VI), and 12 h (VII) are shown. No further change of the absorption spectrum occurs after 12 h. During this 12-h period the absorption in the range of 400–500 nm decays and the absorption around 380 nm increases with an isosbestic point of the transition at 400 nm. The amount of 9-*cis*-retinal in the sample does not change during this period but more 13-*cis*-retinal is formed from all-*trans* due to the dark adaptation process (see Table 1). Due to the shift in the absorption spectrum the release of 9-*cis*-retinal from the Schiff base linkage and the formation of the 380-nm absorbing product is assumed as reported upon neutralization of the 490-nm absorbing photoproduct of acidified BR (Fischer et al., 1981). This correlates with numerical simulations where a constant decomposition rate of the 490-nm to the 380-nm 9-*cis*-product is assumed. In addition to the change around 380 nm a change in absorption around 570 nm also occurs indicating dark 13-*cis* to all-*trans* transition reverting potential shifts of that isomeric equilibrium.

Finally, the sample was illuminated for 22 min with light of wavelength 532 nm at an intensity of 88 mW/cm^2 followed by a 2-min irradiation from a halogene lamp with light above 300 nm at an intensity of 400 mW/cm^2 (Fig. 9 *E*). The absorption at 560 nm increased under the monochromatic excitation with the laser (Fig. 9 *E*, VIII) but the absorption at 380 nm remained unchanged. However, second illumination with white light resulted in an almost complete disappearance of this part and a further increase of the 560-nm absorption. According to the analysis of the retinal isomer composition, the monochromatic excitation at 532 nm reconverts the remaining 490-nm product but leaves the 380-nm product unchanged (Table 1, EVIII and EIX). Except for a very small part (compare I – IX in Fig. 9 *F*) all photoproducts were reconverted to the initial state of the BR film by illumination with additional white light. This is expected from the experience with the photochemical behaviour of free retinal (Fischer et al., 1981) and photoproducts of BR (Szundi and Stoeckenius, 1989; Chang et al., 1987; Chang et al., 1988; Liu and Ebrey, 1987; Szundi and Stoeckenius, 1988).

TABLE 1 Retinal composition of BT_{WT} films after exposures according to Fig. 9

Absorption spectrum	Retinal composition	13-*cis*	9-*cis*	all-*trans*
			%	
AI	Light-adapted: 5 min 400 mW/cm² with arclamp	11	<1	89
AIV	+5 min 500 mW/cm² at 676 nm	16	22	62
CVII	+12 h in the dark	24	20	56
EVIII	+5 min 300 mW/cm² at 532 nm	31	10	59
EIX	+5 min 400 mW/cm² with arclamp	20	3	77

The accuracy of the retinal extraction data is estimated to ±3% of the given values due to the statistical errors in the extraction analysis and slight differences of the used BR films. The light/dark-adaptation depends on the humidity of the BR films (Korenstein and Hess, 1977). Also it was reported that photoconversion into the dark-adapted state occurs with wavelengths on the red wing (Kouyama et al., 1985). Therefore the 13-*cis*:all-*trans* ratios cannot be assigned clearly to dark- or light-adapted BR.

In summary the result of the above described experiments is that the photochemical formation of a 9-*cis*-retinal containing species occurs under constant irradiation with red light without the presence of blue membrane as a starting material. This 9-*cis* material is photochemically reconvertable to all-*trans*, but thermally stable in the range of hours. This primary 9-*cis* photoproduct P is converted thermally very slowly into a species with maximal absorption at 380 nm. Apparently the Schiff base linkage to Lys-216 (Bayley et al., 1981; Katre et al., 1981; Lemke and Oesterhelt, 1981) is hydrolyzed and free 9-*cis*-retinal is formed in the binding site of BR (Q-state) and which then shows long-term stability. Also this species can be photochemically reconverted to 13-*cis*/all-*trans* BR as reported for mixtures of 9-*cis*-retinal and bacterio-opsin (Oesterhelt and Schuhman, 1974).

The meaning of O-photochemistry for optical applications of BR films

Important for optical and holographic applications of BR films is the finding that extended irradiation with wavelengths in the far red leads to the formation of long-living thermally stable products.

In applications where the dynamic properties of BR films are required, e.g., optical processing, the formation of long-living products can easily be suppressed. In all cases where green-yellow background irradiance is applied, e.g., M-type holograms, effective photochemical reconversions of the P- and Q-states to the initial B-state is guaranteed and no net loss of photoactive material out of the common all-*trans*/13-*cis* cycle occurs.

However, there are some possible applications where this phototransition may be advantageous. The all-*trans*/9-*cis* photosystem contains the key feature for short-term and long-term storage of information, i.e., the absence of a thermal pathway to all-*trans*/13-*cis* BR. For example the O → P phototransition may be used in the way that a hologram recorded with green-yellow light can be photochemically fixated by an intense pulse of 670–690-nm light with a duration shorter than the cycle time from B → O (millisecond range). Only in the bright regions of the initial B-type hologram a relevant population of the O-state does occur and the 670–690-nm pulse leads to the formation of the photoproducts of O, and thus a photochemical fixation of the primary hologram can be obtained. Illumination with a shorter wavelength, e.g., in the green range, releases the material from the P-state. This procedure is in analogy to an experimental approach by Hwang et al. (1978) for the investigation of the O-state kinetics. However, they did not observe the branching of the photocycle.

Finally "long-term" storage of information is possible in the P-state and its final product Q, which both are photoerasable and therefore mark the way to the use of BR at ambient pH values as a long-term information storage material.

DISCUSSION

The results reported here document the photochemical activity of the O-state in bacteriorhodopsin for the first time. The photoproduct P contains a 9-*cis*-retinal configuration. It decays thermally into the final product Q which contains free 9-*cis*-retinal in the binding site. Both states P and Q are photochemically reconvertible to the B state. This allows dynamic holography (O-type hologram) with BR_{WT} where holograms can be photochemically fixed and erased at will. At the same time information can be stored on a long time basis.

Formation of 9-*cis*-retinal has been first observed by irradiation of acidified purple membranes (Oesterhelt and Stoeckenius, 1971) which are blue (Fischer et al., 1981; Fischer and Oesterhelt, 1979). Blue membranes (or BR605) can be obtained from purple membranes either at low pH values (Oesterhelt and Stoeckenius, 1971; Maeda and Yoshizawa, 1980; Fischer et al., 1981; Szundi and Stoeckenius, 1989), by removal of divalent cations (Chang et al., 1987; Chang et al., 1988; Liu and Ebrey, 1987), in a special lipid environment (Szundi and Stoeckenius, 1988), by low tenside concentrations (Padros et al., 1984) or by mutation of Asp^{85} to either glutamic acid (Subramaniam et al., 1990; Lanyi et al., 1992) or any nonacidic amino acid side chain (Otto et al., 1990). Early experimental results had suggested that the blue color of acidified BR (BR605) is due to a protonation of the counterion of the Schiff base (Fischer and

Oesterhelt, 1979; Mowery et al., 1979). This negative charge was identified as a complex anion (de Groot et al., 1989a; de Groot et al., 1989b) which includes Asp^{85} as an important component. Acidification of BR below pH 3 causes the blue color and by NMR it has been shown that only water exposed carboxylgroups are protonated at low pH (Gerwert et al., 1987). Since the Schiff base exchanges protons with the aqueous phase (Harbison et al., 1988) and the extracellular half channel of BR is wider than the cytoplasmic half channel (Henderson et al., 1990) it seems likely that Asp^{85} is protonated during acidification causing the blue color. A more direct evidence has been obtained in mutated BR_{D85E} which has a drastic upward shift in pK of the blue to purple transition (Subramaniam et al., 1990; Lanyi et al., 1992). The color shift leading from an inactive to an active proton pump has been linked to the deprotonation of the glutamic acid in position 85 (Fahmy et al., 1992) and Asp^{85} is the only internal carboxyl group that becomes protonated in the M state of the photocycle (Metz et al., 1992). Generalizing the blue color of BR can be explained by the removal of the negative charge in position 85, either by shifting the pK of the carboxyl group by protonation during the photocycle or by removing this group all together. This situation is found in halorhodopsin (HR) which does not have either a proton donor or acceptor because it is a chloride pump. The surprising similarity of both proteins might be seen in the fact, that 9-*cis*-retinal formation under red light exposure has been reported in HR (Zimanyi and Lanyi, 1987).

In accordance with this all blue BR species were found to be inactive proton pumps and no M could be observed (Lanyi et al., 1992). The dominant photoreaction of BR605 is a transition to an L-type intermediate which persists for a time roughly equal to the lifetime of M at neutral pH before returning to the initial state (Varo and Lanyi, 1989). Extended exposure of either BR605 or decationized blue membrane to red light results in the formation of a so-called pink membrane which contains 9-*cis*-retinal and has an absorption maximum at 491 nm and an extinction coefficient of 44.500 1 mol^{-1} cm^{-1} (Chang et al., 1987; Liu and Ebrey, 1987; Fischer et al., 1981; Pande et al., 1986; Maeda and Yoshizawa, 1980). In addition 11-*cis*-retinal absorbing maximally at 560 nm was found in irradiated acidified purple membranes in 67% glycerol (Maeda and Yoshizawa, 1980). The quantum efficiency of the photoconversion of the blue (all-*trans*) to the pink (9-*cis*) form was determined to be 1.6×10^{-4}. For the pink to blue photoconversion a 55 times higher value of 8.8×10^{-3} was reported (Liu and Ebrey, 1987). The pink form is regarded to be thermally stable (Liu and Ebrey, 1987) at low pH but during neutralization release of free 9-*cis*-retinal in the binding site was observed and so-called BR380 is formed (Fischer et al., 1981).

A contribution of photoproducts of the residual 13-*cis*-BR in the films (see Table 1) involving its bathoproduct which absorbs maximally at 610 nm (Kalinksy et al., 1977; Iwasa et al., 1981) cannot be excluded but the amount 9-*cis*-retinal formed (see Table 1) indicates its origin from the larger all-*trans* pool.

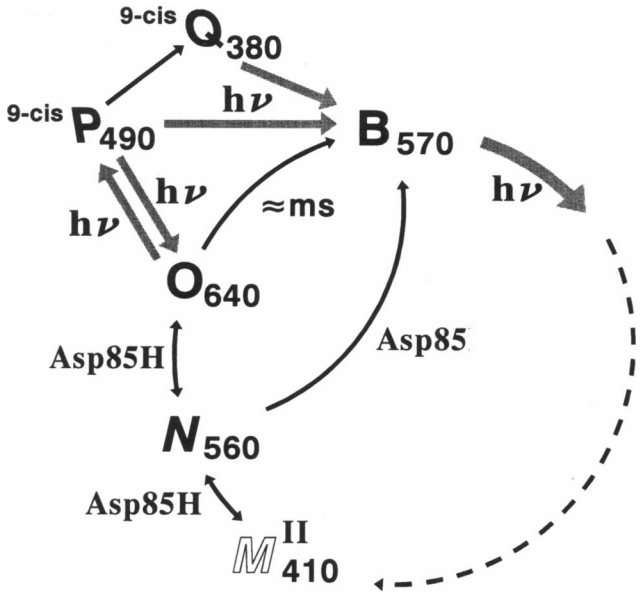

FIGURE 10 Suggested model for the thermal and photochemical conversions of the late photocycle intermediates of BR_{WT}. When N is formed from M and aspartic acid 85 is deprotonated (Asp^{85}) in the meantime BR returns to the B-state directly from the N-state. The O-state is formed only when aspartic acid 85 is still protonated ($Asp^{85}H$). From the all-*trans*-retinal configuration of O a photoproduct is formed in a photochemical transition induced with red light. This state P is characterized by its 9-*cis*-retinal configuration and maximal absorption at 490 nm. In the dark a thermal decomposition of the P-state (9-*cis*-retinal attached to Lys^{216}) into the Q product is observed. The Q product presumably contains free 9-*cis*-retinal in the binding site. Photochemical excitation of the P- and Q-state lead to the regeneration of all-*trans*-retinal and its linkage to the bacterio-opsin. Depending on the protonation state of aspartic acid 85 the photochemical reconversion leads to the O- or B-state. No net loss of photoactive material (13-*cis* ⇄ all-*trans*) occurs due to the O → P pathway. Material is only temporarily trapped/stored in the 9-*cis* state(s).

The O-state of BR and BR605 are spectroscopically very similar when comparing their respective difference spectra with BR (Fischer and Oesterhelt, 1979; Lam et al., 1982). Both occur in all-*trans* configuration of their chromophores (Smith et al., 1983; Fischer and Oesterhelt, 1979) and for the O-state it has recently been shown that Asp^{85} is protonated (Mueller et al., 1991) and releases the proton through the extracellular channel during the transition to BR in completion of the photocycle. This way Asp^{85} fulfills its role as proton acceptor in the extracellular channel receiving it from the Schiff's base upon M formation and finally transferring it to the medium.

A straightforward interpretation of these results is that an already protonated acceptor Asp^{85} prevents M formation, i.e., release of the proton from the Schiff base, and causes a short circuited photocycle. At the same time it allows for a photoisomerization to 9-*cis*-retinal with low quantum yield. Thus, a change in charge around the Schiff base allows for a side reaction of the otherwise exclusive thermoreversible all-*trans* → 13-*cis* photoisomerization.

Under physiological conditions no blue chromophor of the BR605 type occurs but the O-state of BR as an intermediate of the standard photocycle apparently has exactly the same

properties as BR605. We don't know whether it also has a short circuited photocycle in the ms range leading from O to O, but our results clearly show the formation of the 9-*cis* configuration. Under physiological conditions this reaction would be without importance because it has a low quantum yield, only low photostationary O-state concentrations occur and the products of O show photochemical reversibility. In fact we observed appreciable P formation in BR films presumably because the O-state is selectively accumulated due to low proton mobility in the medium. After reprotonation of M ($M^{II} \rightarrow N$) (Fig. 10) *cis* → *trans* isomerization and deprotonation of Asp^{85} occur simultaneously. If the latter reaction is fast (high pH, high proton mobility) no O-intermediate is observed but only the N → BR transition. If the deprotonation is slow the O-state (all-*trans* and protonated Asp^{85}) is passed.

Upon formation of P from O a 9-*cis* configuration of retinal is created in an neutral pH environment. This condition causes a slow transition to Q with a concomitant shift in λ_{max} from 490 to 380 nm. We interpret this as hydrolysis of the Schiff base to free 9-*cis*-retinal in the binding site. This reaction has been observed upon neutralization of the 9-*cis* species produced from acid BR605 (Fischer et al., 1981). Hydrolysis is further likely because 9-*cis*-retinal in bacterioopsin cannot form a Schiff base (Fischer et al., 1981).

As expected P as well as Q can be photochemically reconverted to the all-*trans* state. It is a general property of retinal in BR that isomers are photoconvertible and finally trapped in all-*trans* or 13-*cis*. We do not know which intermediates are passed during that transition but assume that photoisomerization must be the primary reaction. This means that the photoreaction would lead back to the O-state if Asp^{85} is still protonated. Considering the lifetimes of P (or Q), however, we conclude that the B-state is the product.

For optical applications the property of the O-state to allow a photochemical fixation of a primary hologram is most interesting. In principle three methods of improving this material exist: i) modification of the physicochemical conditions of the BR-film in order to obtain a high O-state population; ii) modifications of the primary structure of BR to obtain the same as in method i; iii) modification of the primary structure to create a blue membrane with the properties described for O or acidic BR (BR605).

Here we have shown the feasibility of method i. Mutations have been created which indeed show drastically enhanced photostationary O concentration at neutral pH by replacing Leu^{83} by Ala or Thr (Subramaniam et al., 1991). This demonstrates feasibility of method ii. Finally, several mutations are known such as D85E, N, or T which produce no M intermediate but an L-type intermediate. If it is possible to write short time information into this L form absorbing around 560 nm, i.e., 50-nm blue-shifted from the initial state, long time irradiation leading to 9-*cis* would permanently fixate this information, but it would be photoerasable as described. Thus, also method iii seems feasible. Only experimental optimization will finally determine practical realization of BR. The high potential of BR in biotechnology seems to be demonstrated once more.

Helpful discussions and experimental contributions of Romy Lambrecht and Jörg Tittor are gratefully acknowledged.
This work was supported by the Bundesministerium für Forschung und Technologie (FKZ 0319231B).

REFERENCES

1. Baribeau, J., and F. Boucher. 1985. Isolation, purification, and partial characterization of stable forms of monomeric bacteriorhodopsin in lauryl sucrose. *Can. J. Biochem. Cell Biol.* 63:305–312.
2. Bayley, H., K.-S. Huang, R. Radhakrishnan, A. H. Ross, Y. Takagaki, and H. G. Khorana. 1981. Site of attachment of retinal in bacteriorhodopsin. *Proc. Natl. Acad. Sci. USA.* 78:2225–2229.
3. Birge, R. R. 1990. Nature of the primary photochemical events in rhodopsin and bacteriorhodopsin. *Biochim. Biophys. Acta.* 1016:293–327.
4. Bräuchle, C., and D. M. Burland. 1983. Holographic methods for the investigation of photochemical and photophysical properties of molecules. *Angew. Chem. Int. Ed. Engl.* 22:582–598.
5. Bräuchle, C., N. Hampp, and D. Oesterhelt. 1991. Optical applications of bacteriorhodopsin and its mutated variants. *Adv. Mater.* 3:420–428.
6. Chang, C. H., S. Y. Liu, R. Jonas, and R. Govindjee. 1987. The pink membrane: the stable photoproduct of deionized purple membrane. *Biophys. J.* 52:617–623.
7. Chang, C. H., R. Jonas, R. Govindjee, and T. G. Ebrey. 1988. Regeneration of blue and purple membranes from deionized bleached membranes of halobacterium halobium. *Photochem. Photobiol.* 47:261–265.
8. de Groot, H. J. M., G. S. Harbison, P. B. Rosenthal, A. C. Kolbert, J. Herzfeld, and R. G. Griffin. 1989a. ^{15}N NMR evidence for a complex Schiff base counterion in bacteriorhodopsin. *Biophys. J.* 55:384*a*. (Abstr.)
9. de Groot, H. J. M., G. S. Harbison, J. Herzfeld, and R. G. Griffin. 1989b. Nuclear magnetic resonance study of the Schiff base in bacteriorhodopsin: counterion effects on the nitrogen-15 shift anisotropy. *Biochemistry.* 28:3346–3353.
10. Drachev, L. A., A. D. Kaulen, V. P. Skulachev, and V. V. Zorina. 1986. Protonation of a novel intermediate P is involved in the M→bR step of the bacteriorhodopsin photocycle. *FEBS Lett.* 209:316–320.
11. Dunn, R. J., N. R. Hackett, J. M. McCoy, B. H. Chao, K. Kimura, and H. G. Khorana. 1987. Structure-function studies on bacteriorhodopsin. I. Expression of the bacterioopsin gene in *Escherichia coli*. *J. Biol. Chem.* 262:9246–9254.
12. Fahmy, K., O. Weidlich, M. Engelhard, J. Tittor, D. Oesterhelt, and F. Siebert. 1992. Identification of the proton acceptor of Schiff base deprotonation in bacteriorhodopsin: a Fourier-transform-infrared study of the mutant Asp^{85}→Glu in its natural lipid environment. *Photochem. Photobiol.* 56:1073–1083.
13. Fischer, U., and D. Oesterhelt. 1979. Chromophore equilibria in bacteriorhodopsin. *Biophys. J.* 28:211–230.
14. Fischer, U. C., P. Towner, and D. Oesterhelt. 1981. Light induced isomerisation, at acidic pH, initiates hydrolysis of bacteriorhodopsin to bacterio-opsin 9-*cis*-retinal. *Photochem. Photobiol.* 33:529–537.
15. Gerwert, K., U. M. Ganter, F. Siebert, and B. Hess. 1987. Only water-exposed carboxyl groups are protonated during the transition to the cation-free blue bacteriorhodopsin. *FEBS Lett.* 213:39–44.
16. Gross, R. B., K. C. Izgi, and R. R. Birge. 1992. Holographic thin films, spatial light modulators and optical associative memories based on bacteriorhodopsin. *Proc. SPIE-Int. Soc. Opt. Eng.* 1662:1–11.
17. Hampp, N., C. Bräuchle, and D. Oesterhelt. 1990. Bacteriorhodopsin wildtype and variant aspartate-96→asparagine as reversible holographic media. *Biophys. J.* 58:83–93.
18. Hampp, N., A. Popp, C. Bräuchle, and D. Oesterhelt. 1992. Diffraction efficiency of bacteriorhodopsin films for holography containing bacteriorhodopsin wildtype BR_{WT} and its variants BR_{D85E} and BR_{D96N}. *J. Phys. Chem.* 96:4679–4685.
19. Harbison, G. S., S. O. Smith, J. A. P. C. Winkel, J. Lugtenberg, J. Herzfeld, R. Mathies, and R. G. Griffin. 1984. Dark-adapted bacteriorhodopsin contains 13-*cis*, 15-syn and all-*trans*, 15-anti retinal

Schiff bases. *Proc. Natl. Acad. Sci. USA.* 81:1706–1709.

20. Harbison, G. S., J. E. Roberts, J. Herzfeld, and R. G. Griffin. 1988. Solid-state NMR detection of proton exchange between the bacteriorhodopsin Schiff base and bulk water. *J. Am. Chem. Soc.* 110:7221–7223.
21. Haronian, D., and A. Lewis. 1991. Elements of a unique bacteriorhodopsin neural network architecture. *Appl. Opt.* 30:597–608.
22. Henderson, R., J. M. Baldwin, T. A. Ceska, F. Zemlin, E. Beckmann, and K. H. Downing. 1990. Model for the structure of bacteriorhodopsin based on high-resolution electron cryomicroscopy. *J. Mol. Biol.* 213: 899–929.
23. Hwang, S. B., J. I. Korenbrot, and W. Stoeckenius. 1978. Transient photovoltages in purple membrane multilayers charge displacement in bacteriorhodopsin and its photointermediates. *Biochim. Biophys. Acta.* 509:300–317.
24. Iwasa, T., F. Tokunaga, and T. Yoshizawa. 1981. Photochemical reaction of 13-*cis* bacteriorhodopsin studied by low temperature spectrophotometry. *Photochem. Photobiol.* 33:539–545.
25. Kalinsky, O., C. R. Goldschmidt, and M. Ottolenghi. 1977. On the photocycle and light adaptation of dark-adapted bacteriorhodopsin. *Biophys. J.* 19:185–189.
26. Katre, N. V., P. K. Wolber, W. Stoeckenius, and R. M. Stroud. 1981. Attachment site(s) of retinal in bacteriorhodopsin. *Proc. Natl. Acad. Sci. USA.* 78:4068–4072.
27. Kogelnik, H. 1969. Coupled wave theory for thick hologram gratings. *Bell Syst. Tech. J.* 48:2909–2947.
28. Korenstein, R., and B. Hess. 1977. Hydration effects on *cis-trans* isomerization of bacteriorhodopsin. *FEBS Lett.* 82:7–11.
29. Kouyama, T., R. A. Bogomolni, and W. Stoeckenius. 1985. Photoconversion from the light-adapted to the dark-adapted state of bacteriorhodopsin. *Biophys. J.* 48:201–208.
30. Kouyama, T., K. Kinosita, and A. Ikegami. 1988. Structure and function of bacteriorhodopsin. *Adv. Biophys.* 24:123–175.
31. Lam, E., I. Fry, L. Packer, and Y. Mukohata. 1982. Comparison of the O_{640} photointermediate and acid-induced species in membrane patches from *Halobacterium halobium* S_9 and R_1mW strains. *FEBS Lett.* 146: 106–110.
32. Lanyi, J. K., J. Tittor, G. Varo, G. Krippahl, and D. Oesterhelt. 1992. Influence of the size and protonation state of acidic residue 85 on the absorption spectrum and photoreaction of the bacteriorhodopsin chromophore. *Biochim. Biophys. Acta.* 1099:102–110.
33. Lemke, H. D., and D. Oesterhelt. 1981. Lysine 216 is a binding site of the retinyl moiety in bacteriorhodopsin. *FEBS Lett.* 128:255–260.
34. Liu, S. Y., and T. G. Ebrey. 1987. The quantum efficiency for the interphotoconversion of the blue and pink forms of purple membrane. *Photochem. Photobiol.* 46:263–267.
35. Maeda, A., and T. I. T. Yoshizawa. 1980. Formation of 9-*cis*- and 11-*cis*-retinal pigments from bacteriorhodopsin by irradiating purple membrane in acid. *Biochemistry.* 19:3825–3831.
36. Metz, G., F. Siebert, and M. Engelhard. 1992. Asp^{85} is the only internal aspartic acid that gets protonated in the M intermediate and the purple-to-blue transition of bacteriorhodopsin. *FEBS Lett.* 303:237–241.
37. Miller, A., and D. Oesterhelt. 1990. Kinetic optimization of bacteriorhodopsin by aspartic acid 96 as an internal proton donor. *Biochim. Biophys. Acta.* 1020:57–64.
38. Mowery, P. C., R. H. Lozier, Q. Chae, Y.-W. Tseng, M. Taylor, and W. Stoeckenius. 1979. Effect of acid pH on the absorption spectra and photoreactions of bacteriorhodopsin. *Biochemistry.* 18:4100–4107.
39. Mueller, K. H., H. J. Butt, E. Bamberg, K. Fendler, B. Hess, F. Siebert, and M. Engelhard. 1991. The reaction cycle of bacteriorhodopsin: an analysis using visible absorption, photocurrent and infrared techniques. *Eur. Biophys. J.* 19:241–251.
40. Nassal, M., T. Mogi, S. S. Karnik, and H. G. Khorana. 1987. Structure-function studies on bacteriorhodopsin. III. Total synthesis of a gene for bacterio-opsin and its expression in *Escherichia coli*. *J. Biol. Chem.* 262:9264–9270.
41. Ni, B. F., M. Chang, A. Duschl, J. Lanyi, and R. Needleman. 1990. An efficient system for the synthesis of bacteriorhodopsin in *Halobacterium halobium*. *Gene.* 90:169–172.
42. Oesterhelt, D., and L. Schuhman. 1974. Reconstitution of bacteriorhodopsin. *FEBS Lett.* 44:262–265.
43. Oesterhelt, D., and W. Stoeckenius. 1971. Rhodopsin-like protein from the purple membrane of *Halobacterium halobium*. *Nature (London), New Biol.* 233:149–152.
44. Oesterhelt, D., and W. Stoeckenius. 1974. Isolation of the cell membrane of *Halobacterium halobium* and its fractionation into red and purple membrane. *In* Methods of Enzymology, Biomembranes Part A. S. Fleischer and L. Packer, editors. Academic Press, New York. 667–678.
45. Oesterhelt, D., C. Bräuchle, and N. Hampp. 1991. Bacteriorhodopsin: a biological material for information processing. *Q. Rev. Biophys.* 24: 425–478.
46. Otto, H., T. Marti, M. Holz, T. Mogi, L. J. Stern, F. Engel, H. G. Khorana, and M. P. Heyn. 1990. Substitution of amino acids Asp-85, Asp-212, and Arg-82 in bacteriorhodopsin affects the proton release phase of the pump and the pK of the Schiff base. *Proc. Natl. Acad. Sci. USA.* 87:1018–1022.
47. Padros, E., M. Dunach, and M. Sabes. 1984. Induction of the blue form of bacteriorhodopsin by low concentrations of sodium dodecyl sulfate. *Biochim. Biophys. Acta.* 796:1–7.
48. Pande, C., R. H. Callender, C. H. Chang, and T. G. Ebrey. 1986. Resonance Raman study of the pink membrane photochemically prepared from the deionized blue membrane of *H. halobium*. *Biophys. J.* 50: 545–549.
49. Scherrer, P., M. K. Mathew, W. Sperling, and W. Stoeckenius. 1989. Retinal isomer ratio in dark-adapted purple membrane and bacteriorhodopsin monomers. *Biochemistry.* 28:829–834.
50. Smith, S. O., J. A. Pardoen, P. P. J. Mulder, B. Curry, J. Lugtenburg, and R. Mathies. 1983. Chromophore structure in bacteriorhodopsin's O640 photointermediate. *Biochemistry.* 22:6141–6148.
51. Soppa, J., and D. Oesterhelt. 1989. Bacteriorhodopsin mutants of *Halobacterium* spec. GRB. I. The 5-bromo-2′-desoxyuridine selection as a method to isolate point mutants in *Halobacteria*. *J. Biol. Chem.* 264: 13043–13048.
52. Soppa, J., J. Otomo, J. Straub, J. Tittor, S. Meeβen, and D. Oesterhelt. 1989. Bacteriorhodopsin mutants of *Halobacterium* spec. GRB. II. Characterization of mutants. *J. Biol. Chem.* 264:13049–13056.
53. Steinberg, G., N. Friedman, M. Sheves, and M. Ottolenghi. 1991. Isomer composition and spectra of the dark and light adapted forms of artificial bacteriorhodopsins. *Photochem. Photobiol.* 54:969–976.
54. Subramaniam, S., T. Marti, and H. G. Khorana. 1990. Protonation state of Asp (Glu)-85 regulates the purple-to-blue transition in bacteriorhodopsin mutants Arg-82→Ala and Asp-85→Glu: the blue form is inactive in proton translocation. *Proc. Natl. Acad. Sci. USA.* 87: 1013–1017.
55. Subramaniam, S., D. A. Greenhalgh, P. Rath, K. J. Rothschild, and H. G. Khorana. 1991. Replacement of leucine-93 by alanine or threonine slows down the decay of the N and O intermediates in the photocycle of bacteriorhodopsin: implications for proton uptake and 13-*cis*-retinal→all-*trans*-retinal reisomerization. *Proc. Natl. Acad. Sci. USA.* 88:6873–6877.
56. Szundi, I., and W. Stoeckenius. 1988. Purple-to-blue transition of bacteriorhodopsin in a neutral lipid environment. *Biophys. J.* 54:227–232.
57. Szundi, I., and W. Stoeckenius. 1989. Surface pH controls purple-to-blue transition of bacteriorhodopsin. A theoretical model of purple membrane surface. *Biophys. J.* 56:369–383.
58. Varo, G., and J. K. Lanyi. 1989. Photoreactions of bacteriorhodopsin at acidic pH. *Biophys. J.* 56:1143–1151.
59. Varo, G., and J. K. Lanyi. 1991. Kinetic and spectroscopic evidence for an irreversible step between deprotonation and reprotonation of the Schiff base in the bacteriorhodopsin photocycle. *Biochemistry.* 30:5008–5015.
60. Varo, G., A. Duschl, and J. K. Lanyi. 1990. Interconversions of the M, N, and O intermediates in the bacteriorhodopsin photocycle. *Biochemistry.* 29:3798–3804.
61. Vsevolodov, N. N., G. R. Ivanitskii, M. S. Soskin, and V. B. Taranenko. 1986. Biochrome films: reversible media for optical recording. *Avtometriya.* 2:41–48.
62. Werner, O., B. Fischer, and A. Lewis. 1992. Strong self-defocusing effect and four-wave mixing in bacteriorhodopsin films. *Opt. Lett.* 17: 241–243.
63. Zimanyi, L., and J. K. Lanyi. 1987. Iso-halorhodopsin: a stable, 9-*cis* retinal containing photoproduct of halorhodopsin. *Biophys. J.* 52: 1007–1013.